# ICSO 2016

# International Conference on Space Optics

Biarritz, France

18–21 October 2016

*Edited by Bruno Cugny, Nikos Karafolas and Zoran Sodnik*



## *Laser communication experiments between Sota and Meo optical ground station*

*G Artaud*

*J.-L. Issler*

*N. Védrenne*

*C. Robert*

*et al.*

# LASER COMMUNICATION EXPERIMENTS BETWEEN SOTA AND MEO OPTICAL GROUND STATION

G. Artaud[1], J-L. Issler[1], N. Védrenne[2], C. Robert[2], C. Petit[2], E. Samain[3], D-H. Phung[3], N. Maurice[3], M. Toyoshima[4], D. Kolev[4]

[1]CNES, France; .[2]ONERA, France, [3]Observatoire de la Cote d'azur and CNRS, France, [4]NICT, Japan

## INTRODUCTION

Optical transmissions between earth and space have been identified as key technologies for future high data rate transmissions between satellites and ground. CNES is investigating the use of optics both for High data rate direct to Earth transfer from observation satellites in LEO, and for future telecommunications applications using optics for the high capacity Gateway link.

In order to assess the feasibility of these future systems, several studies have been initiated for investigating the propagation channel and its impact on the data transmissions. The aim is to define the more appropriate physical layer, in terms of choice of modulations, coding and interleaving, so that to obtain a robust data link.

In order to design future optical transmission systems, field measurements are necessary to confront models with real conditions. The DOMINO project, which stands for "Demonstrator for Optical transMission at hIgh data rate iN Orbit)", aims at performing field measurements with international partners.

Several free space optical communication campaign were performed in 2105 between the NICT SOTA [1] [2], (Small Optical TrAnsponder) instrument  flying on the Low Earth Orbit satellite SOCRATES and the Optical Ground Station (OGS) MeO belonging to Observatoire de la Côte d'Azur (OCA) – GeoAzur. [3].

A new opportunity of campaign arises with the possibility to communicate with OPALS on-board ISS [9].

This paper presents new developments and results that have been obtained in the frame of the DOMINO project.

## I. DOMINO DEMONSTRATOR

The DOMINO project (Demonstrator for Optical transMission at hIgh data rate iN Orbit) is conducted in collaboration between CNES, the Cote d'Azur observatory (Geoazur‑OCA), ONERA, also with participation of Airbus Defense & Space and Thales Alenia Space, and international partners: the National Institute of Information and Communications Technology (NICT), and NASA. Geoazur is the project general contractor. DOMINO project aims at demonstrating the feasibility of free-space optical communication by studying links between optical terminal on-board space vehicles and the MeO station [10], located at Caussols, France.

The MeO station is a versatile telescope used for various laser applications including artificial satellites and lunar laser ranging, optical time transfer, high resolution imaging and debris detection. The MeO telescope (Fig 6) has been upgraded in order to be able to take part in laser telecommunications experiments. An uplink beacon has been added to the telescope, together with a receiver bench and a dedicated instrumentation used to monitor the link [3]. The telescope was already equipped with an Adaptive Optics (AO) bench called ODDISEE. The ODISSEE AO bench has been designed and integrated by ONERA at the Coudé focus of MeO [7] for investigation of various applications, including visible imaging. It was opportunely used during laser links to perform propagation channel analysis using the wavefront sensor (chapter II) and to test injection into Single Mode Fiber (SMF) (see chapter III). The 1.5-m telescope is installed on an Alt-Az mount allowing target tracking up to 5 deg∕s, its tracking performances are presented in chapter V.

The main challenges of the project are the implementation of a complete laser communication from space to ground and the characterization of the turbulent atmosphere during the optical data transfer.

In 2015, five links have been successfully established with SOTA [1] [2] on-board SOCRATES microsatellite. In 2016, the MeO station has been upgraded in order to be able to communicate with OPALS on-board ISS [9] and new developments in adaptive optics were performed by ONERA.

## II. PROPAGATION CHANNEL STUDY

The technology readiness level of optical transmissions between space and earth is quite low even if it takes benefit from very mature optical components used in fiber ground communications and it reuses mastered optical technologies developed for imagery. It can be explained by the specificities of the optical propagation channel that impairs the optical signal, and implies the use of dedicated solutions.

High data rate optical transmissions between space and earth can capitalize on ground communication fiber technologies (preamplifier, wavelength multiplexing, …). However the use of these technologies implies to couple the received signal into single mode fibers, which means to handle a wave front that has a good spatial coherence to maximize coupling efficiency in the fiber. But this coherence is compromised by the impairments caused by the propagation channel in particular by turbulences. To improve the spatial coherence, the use of Adaptive Optics system (AO) is needed before injection into the single mode fiber amplifier receiver. The

complexity of the Adaptive Optics systems and the choice of parameters are directly dependent on the atmospheric turbulences and the optical physical layer (modulations, coding, interleaving).

There is a need to improve the knowledge of the propagation channel and much effort has been dedicated to that topic. The atmospheric turbulences simulator TURANDOT has been developed by ONERA for CNES for this purpose. It is an automatically parameterized version of a phase screen numerical model [6] that is dedicated to ground-satellite laser communications. It has been validated with regards to numerical models but also against real measurements of OICETS [5]. The model has been validated at low elevation down to 10°, where there are strong turbulences and analytical models are no more valid, by measuring turbulence profiles on stars [7].

In order to obtain real turbulence profiles to use with the simulation tools and to have a better understanding of the physical phenomena, real measurement campaign are needed. A great opportunity was offered to CNES to take part of the SOTA international campaign [2] that has permitted to collect real turbulence profiles.

The analysis of the pass of the 21th of July 2015 has been already published [11]. The signal was collected using the Shack–Hartmann wavefront sensor (SH-WFS) of the ODISSEE Adaptive Optics Bench. The exploitation of the temporal spectra (PSD) of the wavefront decomposed onto Zernike polynomials enables to retrieve the parameters of $C_n^2$ profile models. In [11] a Multi-Gaussian (MG) $C_n^2$ profile has been used to fit the data recorded in July. This MG profile is plotted in Fig. 1 in black. Several physical parametric profiles are now under study to investigate their potential benefit to fit the data. Results obtained on the WFS data recorded in July for 32.6° elevation, using the MG profile and a HAP [14] profile modified with the addition of two discrete layers, are illustrated in Fig. 2 (left and center). The modified HAP profile seems to provide better fit to the data. First analysis of data gathered in October 2015 with a similar HAP based profile model (results shown in Fig.2 on the right) consolidates the relevancy of such a model. The first profiles extracted from these data are plotted in Fig. 1. The significant difference between July and October HAP based profiles for high altitude layers (above 1 km) could be due to seasonal variations of the turbulence in the free atmosphere. These results however must be consolidated by a systematic analysis that is currently on going.
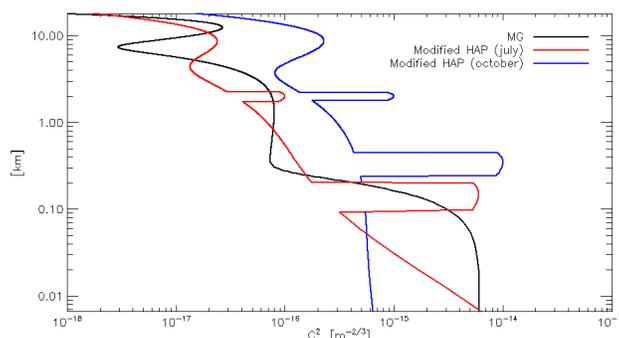


**Fig. 1.** Various $C_n^2$ profiles used in the analytical temporal PSD calculation. Custom $C_n^2$ multi-Gaussian profile for 21st July, more physical $C_n^2$ profiles based on HAP applied for 21st July and 21st October.
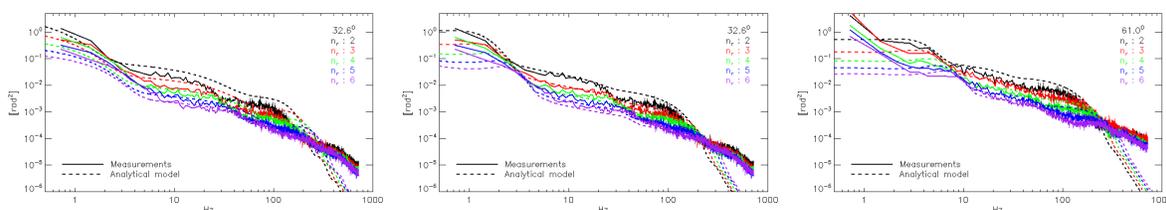


**Fig. 2.** Temporal PSD computed with an analytical model (dashed lines) compared to measurements (continuous lines) for radial orders 2 to 6. Elevations are respectively 32.6-deg for July (at left and center) and 61.0-deg for October (at right).

## III. ADAPTIVE OPTICS

### A. AO bench at 976nm 1,5m pupil

The ODISSEE Adaptive Optics bench has been used on SOTA signal for the two passes of 21th of July 2015 and 15th of October 2015. The analysis of the pass of July has already been published in [11]. The measured performance of the AO was compared to the theoretical one taking into account the characteristics of the bench, the pupil size and the turbulence conditions. During this first test, no SMF module was available and performance relied on focal images analysis The size of the pupil being quite large (1,5m) compared to the fried parameter (r0 goes from 4.5 cm at 500 nm to 6 cm during acquisitions) the AO was not very performant but still

provides a significant improvement. Long exposure images obtained in open and closed AO loop, showed a factor 45 in maximum intensity and ~7 in FWHM. The evaluation of a pseudo-coupling efficiency related to power in the bucket (PIB) gave a 8,8% coupling efficiency instead of 0.6% value in open loop in agreement with numerical simulation of the expected performance of the bench.

*Single Mode Fiber injection experiment*

During the pass of 15th of October 2015, an experiment was performed in order to couple the received signal into a single mode fiber. The set up (Fig.4) consisted of a simultaneous acquisition of the signal and the single mode fiber output onto the imaging camera. The output of the ODISSEE adaptive bench was split in two parts: a portion of the signal was sent to the imaging camera and the other part was injected into a single mode fiber. The signal level at the output of the AO bench was too low to be able to sample the output of the single mode fiber using a detector. The set-up that was used consisted in measuring the average power coupled into the single mode fiber by imaging the output of the fiber onto the imaging camera. Figure 3 shows the imaging camera when a synthetic internal laser source is used to calibrate the experiment (right picture), and the signal received from SOTA (left open loop, center closed loop). For each picture, the PSF of the signal is shown on the left and at the right the small spot shows the power at the output of the single mode fiber. In open loop, due to pointing residuals the PSF of the signal is out of the Field of View of the camera, in closed loop, the signal injected into the single mode fiber can be seen. Considering the pupil size (1,5m) and the fried parameter during the pass (r0 ~ 7 cm @ 976 nm), the theoretical coupling efficiency was estimated to 4,1 %, the measured coupling efficiency was 2,1%, which is a poor coupling efficiency due to high turbulence residuals.
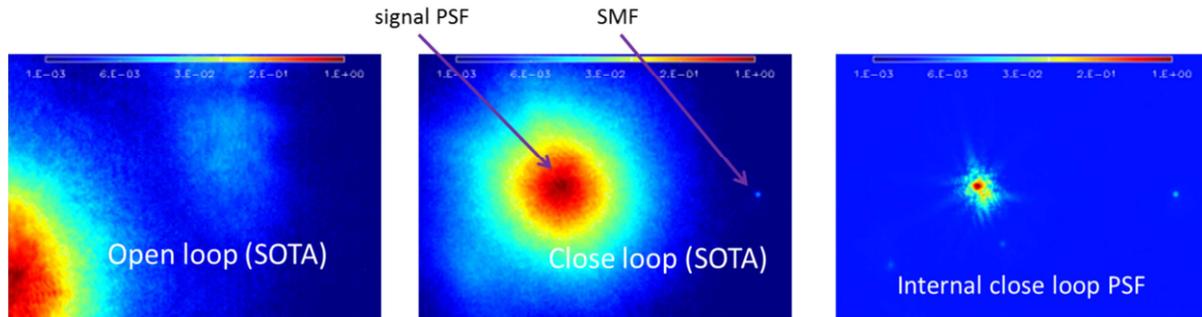


**Fig. 3.** Imaging camera: SOTA signal PSF in open loop (left), SOTA signal PSF in closed loop and SMF (center), internal source used for calibration PSF and SMF (right)
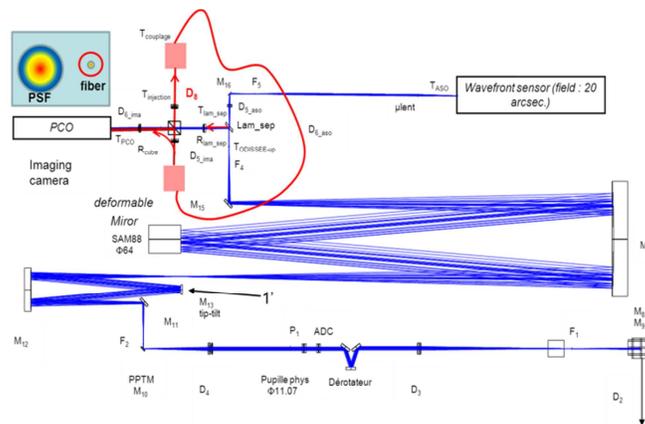


**Fig. 4.** Set-up used for fiber injection experiment using ODISEE AO Bench

*B.   AO bench at 976 nm 40 cm pupil*

In order to improve the coupling efficiency it is needed to reduce the size of the pupil from 1.54 meter to about 40 cm. Indeed the ODISSEE adaptive optics bench performance is not suited for the full pupil and the coupling efficiency will improve greatly by reducing it. A new set-up was consequently prepared for the scheduled SOTA passes of March 2016. A pupil of 40cm was selected in the useful aperture of the 1.54m telescope. The ODISSEE bench was modified in order to scale the Deformable Mirror (DM) and SH-WFS subaperture grid to cover the selected 40cm pupil (see figure 5 center picture). The SMF injection mechanism has also been improved using the CESAR module provided by the Lagrange Laboratory [13].
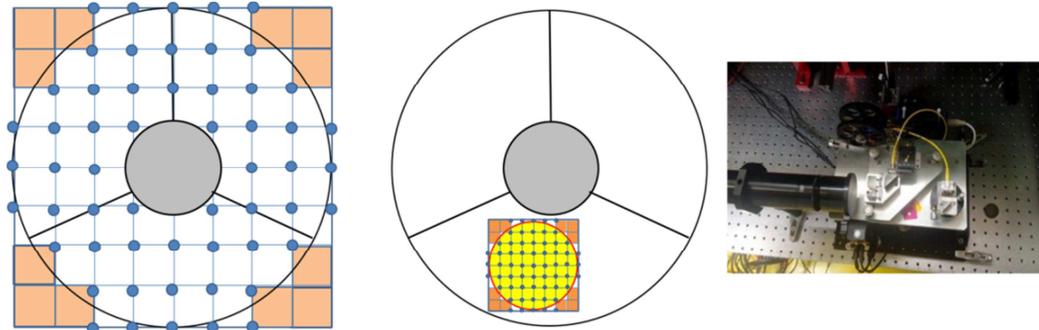
**Fig. 5**. Schematic of the DM actuator grid (dots), located at the angles of SH-WFS subaperture grid (squares). The useful aperture, with telescope spider and central occultation are delimited in black. A 8 × 8 subaperture grid is used on SH-WFS, valid subapertures are whitened [left picture]; DM actuator grid when used on the 40cm pupil taken in the useful aperture of the 1.54m telescope corresponding to the new set-up [middle picture]; CESAR SMF injection module [right picture]

During the planned passes of March 2016, the weather was unfortunately cloudy and even if SOTA sporadically detected the uplink beacon, the telecom laser was not received at the OGS and no acquisition was possible with the new AO set-up.

*C. AO bench at 1550 nm 40c m pupil*

The ODISSEE Adaptive Optics bench could not be used to receive signal at 1550 nm due to the Coudé of the MeO telescope that contains 2 mirrors that do not allow 1550 nm wavelength to pass. A new small adaptive optics bench has been developed and integrated by ONERA. It has been installed at the Nasmyth of the MeO telescope and it is intended to be used on SOTA links and OPALS links. The wave front sensor runs at 2.2kHz and the deformable mirror has 97 actuators.

As for ODISSEE, the usefull aperture at the telescope level has been reduced to 40 cm to be representative of laser communication systems.

ONERA named it: "MéO NAsmyth LIght Small and Automated adaptive optics bench" (MONA-LISA). In the Figure 6, the AO bench can be seen at the left (30 x 60 cm wide) and the DOMINO bench at the right that contains the acquisition and tracking camera and the telecommunication detector. The loop has been closed on stars, and we are waiting for a first opportunity to use it on satellite laser link. On Fig 6 the wavefront variance per Zernike polynomial radial order in open loop and in closed loop is shown for the Star Arcturus at 52° elevation during night.
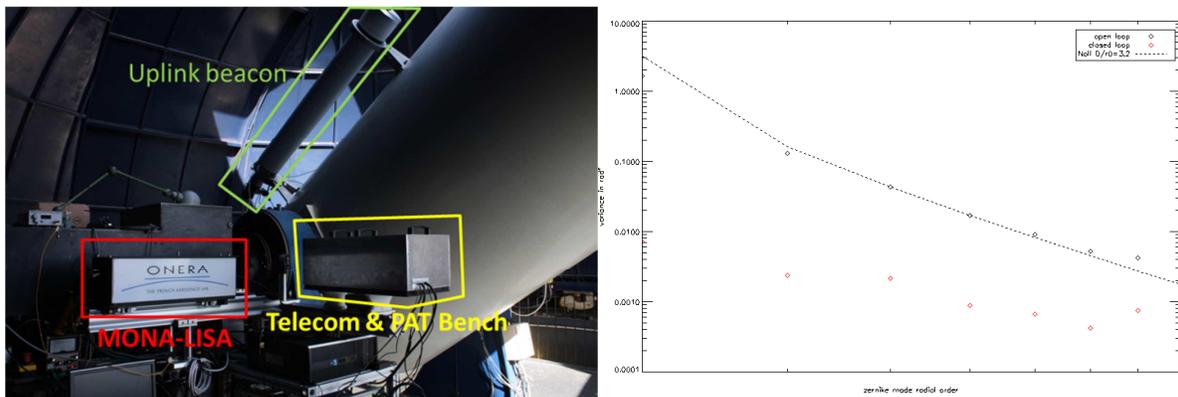


**Fig. 6**. MOLA-LISA AO Bench at nasmyth table [left]. Wavefront variance per Zernike polynomial radial order in open loop ( black square) and in closed loop (red square) measured on a star [right]

## IV. COMMUNICATION RECEIVER

The telecom detection chain used for the OPALS experiment is a modification of the mono-pixel sensor initially designed for SOTA links [3]. It is made with an InGaAs avalanche photodiode, a low noise trans-impedance amplifier and two amplification channels for both telecom and scintillation detections. As compared to SOTA configuration, the bandwidth of the telecom channel is increased by a factor 5 for a telecom bit rate from 10 Mbps for SOTA to 50 Mbps for OPALS. To achieve this objective 2 modifications are made on the sensor: the initial 16 MHz fifth order LC Tchebychev passive filter is removed, and the gain of the trans-impedance amplifier is decreased by a factor 3. The scintillation channel, actively and passively filtered with respectively a

10 kHz second order Sallen-Key filter and a 10 kHz fifth order LC Tchebychev filter, is not modified for the OPALS configuration. The figure 7 is an illustration of the temporal response of the telecom channel of the sensor for the OPALS configuration. The rising and falling edge response is 7 ns.
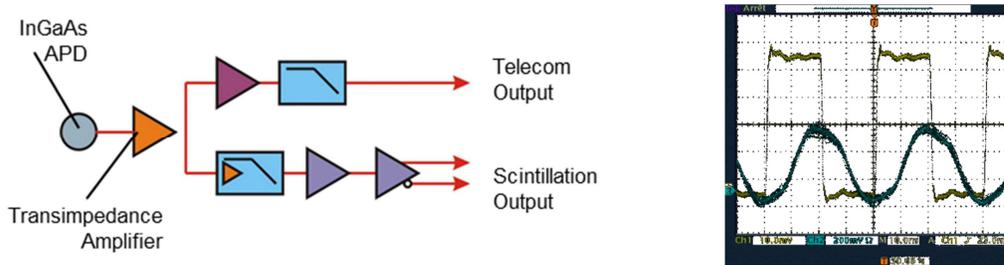


**Fig. 7**. [left]: Monopixel Detector used for both telecom detection and scintillation measurement; [right]:Temporal response of the detector modified for OPALS:green Optical 50 MHz square signal (reference), blue : APD response

### V. MeO Telescope tracking accuracy

The tracking accuracy using auto tracking algorithm of the MeO telescope has been measured on different targets: stars, visible satellites, Satellite SOTA laser links and visible ISS.

*A. SOTA tracking of Meo Telescope*

For the 5 SOTA passes, the Hamamatsu camera (Hamamatsu InGaAs camera G11097-0707S, 128×128 pixels, field of view of 100 arcsec) was used for tracking. The auto tracking system was used only on the first pass of 22nd of June, for the other passes a manual correction of the tracking was performed. The reason of this choice is that the image of the SOTA laser spot on the Hamamatsu camera was not clean enough. Indeed the spot size is large and the beam splitter between the tracking camera and the telecom detector introduces a double reflection that creates a second spot introducing a bias of about 2.5 arcsec on Y axis on the camera (see fig 8 left).
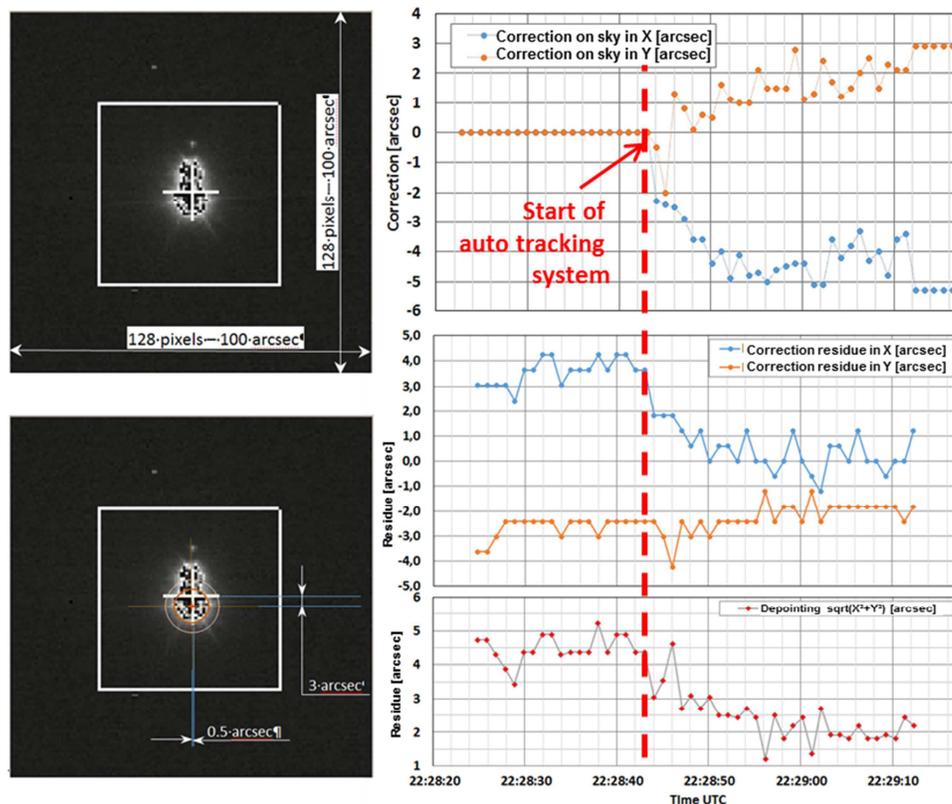


**Fig. 8**. [left] Image of the laser beam from SOTA on the Hammamatsu tracking camera with auto tracking system activated; [right] corrections and residual error using auto tracking for the 22nd of June 2015 pass

For the pass of the 22$^{nd}$ of June, the correction on sky applied on X and Y axis are presented in figure 8 top right. From this curve it can be deduced that the precision of the orbit prediction provided by NICT for the pass was smaller than 7 arcsec. The correction is computed by the algorithm by measuring the delta between the central point of the camera and the spot position. After auto tracking activation at 22:28:43, corrections are applied to the telescope and the tracking residual error decreases from 4.2 arcsec to about 0 on X axis and from -3.7 arcsec to about 2 arcsec in Y axis, leading to a mispointing of about 2.5 arcsec in mean and 1,5 arcsec peak to valley. The performance of the auto tracking system is obtained by measuring the difference between the set point (center of the camera) and the position of the spot after the correction is applied.

For the other 4 passes, the tracking correction were manual, this provides a better tracking accuracy since there is no parasitic image that bias the tracking on Y axis. A summary of some tracking performance of MeO telescope in auto tracking and manual tracking for different targets is presented in Table 1.

**Table 1**. tracking performance of MeO telescope in auto tracking and manual tracking for different targets

| | Auto tracking system | | | Manual tracking correction | | | |
|---|---|---|---|---|---|---|---|
| | Depointing [arcsec] | | TLE[arcsec] | | Depointing [arcsec] | | TLE[arcsec] |
| **Target** | Mean | Peak to valley | Max error | **SOTA** | Mean | Peak to valley | Max error |
| Star | 1,5 | 2.0 | | 22/6 | 1.0 | 2,4 | 13 |
| Sat Jason 2 | 1 | 2,5 | 91 | 28/6 | 2,0 | 4,0 | 25 |
| SOTA 21/6 | 2,5 | 1,5 | 7 | 21/7 | 1,0 | 1,5 | 18 |

*A. ISS auto tracking of Meo Telescope*

This chapter characterizes the performance of Meo telescope on ISS auto tracking. The test was performed on June 09 2016 with ISS pass starting at 22:27:57 (4.52° elevation), culmination at 70.4°. ISS was illuminated by the sun from the beginning to 21:32:44 (4.52° elevation – culmination – 55.8 elevation). The auto tracking was activated when ISS image appears on OGS tracking Hamamatsu camera. The main upgrade concerning the auto tracking system for OPALS compared with the one used with SOTA is an improvement of the camera speed from 4 Hz to 20 Hz. A trajectory example of ISS is shown in figure 9.
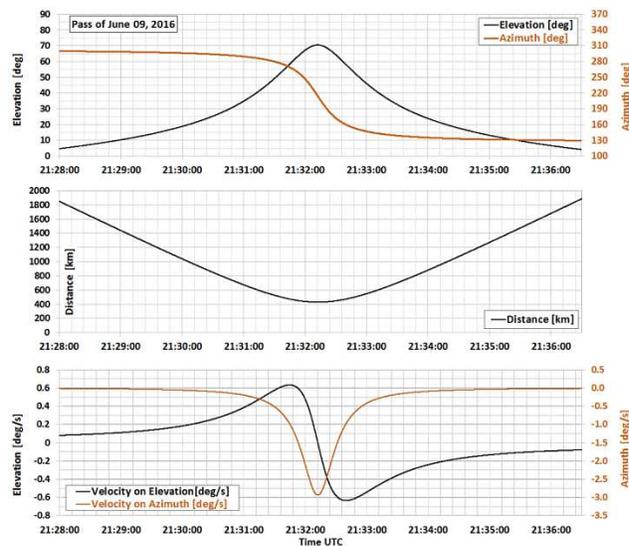


**Fig. 9.** Orbit information of ISS pass for auto tracking test, predicted table is sent by NASA. *Maximal velocity is 3.0 deg/sec on azimuth and 0.65 deg/sec on elevation*
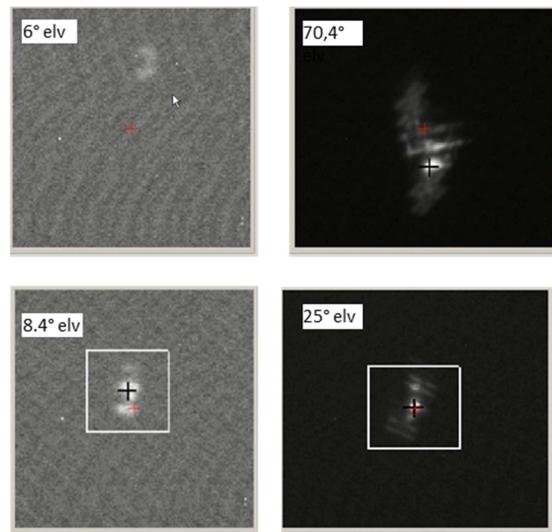


**Fig. 10.** Image of ISS in camera field, auto tracking non-activated (up left) & active (down left), at 25° elevation (down right),and at culmination – 70.4° elevation (up right).

ISS image appeared in camera field at an elevation of 6°, auto tracking is activated at 8.4°. At high elevation, error between predicted and real coordinates is larger than correction capability of the MeO auto tracking system. This is the reason why ISS image was not in the center of camera field at culmination. Fig. 11 shows elevation & azimuth errors between predicted and real coordinates of ISS during the pass when auto tracking is activated. CorrCodHau & CorrCodAz correspond to corrections in Meo telescope coding, CorrX" & CorrY" correspond to corrections on sky or X & Y coordinates of camera.
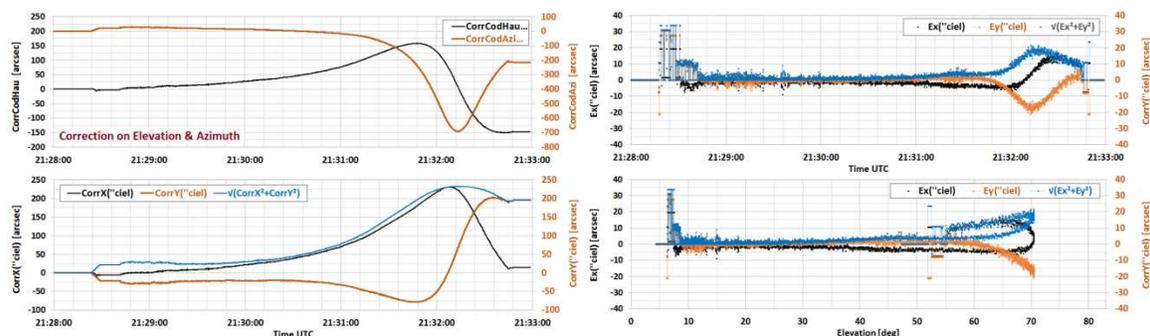
**Fig. 11**. [left] Errors on elevation & azimuth between predicted & real coordinates of ISS, [right] Residual of auto tracking corrections in functions of time & elevation

The maximal corrections on the sky are 230 arcsec & 200 arcsec according to X & Y axis of camera, respectively. The difference between predicted and real coordinates of ISS is maximal at culmination: 230 arcsec (1.2 mrad) @ 70.4° elevation. At low elevation (< 28°), the difference is smaller than 50 arcsec (0.25 mrad). At starting point, when ISS appears in camera field, the difference is about 25 arcsec (0.125 mrad). From these results, one can conclude that uncertainty of NASA prediction is in the range of 1.2 mrad. A beacon beam of 2.0 mrad divergence should be used to cover the prediction uncertainty of ISS.

The residual after auto tracking corrections (Fig 11 right) is smaller than 5 arcsec (25 µrad) on X & Y axis of camera field when elevation of ISS is smaller than 60°, the corresponding difference is smaller than 7 arcsec (35 µrad). At culmination (70.4°), the residual is about 20 arcsec (100 µrad) caused by a large prediction difference and the velocity limitation of the Meo telescope. Larger noise in residuals at low elevation (from 8.4° to 15°) is caused by poor photo-center calculation given by ISS image on camera. When auto tracking is activated (at 8.4° elevation), it needs less than 0.25 sec to eliminate the difference of 10 arcsec (50 µrad).

This preliminary test allowed us to estimate the performance of auto tracking of the Meo telescope with ISS, a residual smaller than 7 arcsec can be obtained when elevation of ISS is smaller than 60°. At very high elevation, a large residual (> 20 arcsec) could cause a misalignment at telecom & scintillation detector which has a field of view of 48 arcsec.

The form of corrections in Meo telescope coding & residual curves match well to those of ISS angular velocities (on elevation and azimuth).
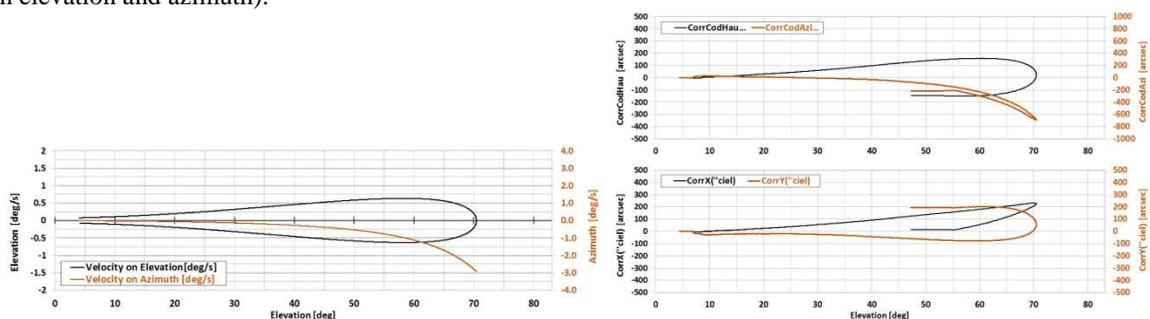


**Fig. 12.** Velocities of ISS on elevation & azimuth in functions of elevation (left), Correction in Meo telescope coding & on sky (X & Y axis of camera) in functions of elevation

**CONCLUSION**

Field measurements are needed in order to improve our knowledge on Free space optical communications between space and Earth. The few links that have been successfully established with SOTA provide valuable insight on link budget and the contributions of pointing and atmospheric turbulences. Having access to a laser link from a satellite enables to assess performances of techniques such as adaptive optics in the conditions of the future system. More experimental links need to be performed in order to obtain more variability on the transmission conditions and be finally able to size future operational laser communication systems for space to ground.

REFERENCES

[1] M. Toyoshima, T. Kuri, W. Klaus, M. Toyoda, H. Takenada, Y. Shoji, Y. Takayama, Y. Koyama, H. Kunimori, T. Jono, S. Yamakawa, K. Arai, "Overview of the Laser Communication System for the NICT Optical Ground Station and Laser Communication Experiments on Ground-to-Satellite Links" Journal of NICT, vol.59, p. 53-75 (2012). [2] .

[2] D. R. Kolev et al., "Overview of International Experiment Campaign with Small Optical TrAnsponder (SOTA)", Proceedings of ICSOS (2015).

[3] E. Samain et al., "First Free Space Optical Communication in Europe Between SOTA and MeO Optical Ground Station", Proceedings of ICSOS (2015).

[5] N. Vedrenne et al. , "Turbulence Effects on Bi-Directional Ground-to-Satellite Laser Communication Systems", Proceedings of ICSO (2012)

[6] M. Sechaud, F. Mahe, T. Fusco, V. Michau, and J.-M. Conan, "High resolution imaging through atmospheric turbulence: link between anisoplanatism and intensity fluctuations," in Optics in Atmospheric Propagation and Adaptive Systems V. Florence, Italy: ESO/SPIE, Sep. 1999, pp. 243–249

[7] N. Vedrenne et al., "Characterization of Atmospheric Turbulence for LEO to Ground Laser Beam Propagation at Low Elevation Angles", Proceedings of ICSOS (2014)

[8] N. Vedrenne et al., "First results of Wavefront sensing on SOTA", Proceedings of ICSOS (2015).

[9] M. J. Abrahamson et al, "OPALS Mission System Operations Architecture for an Optical Communications Demonstration on the ISS", SpaceOps Conferences, 5-9 May 2014, Pasadena, CA

[10] .E. Samain et al., "MeO: the new French lunar laser station", Proceedings of 16th International Workshop on Laser Ranging  - IWLR (2008).

[11] C. Petit, N. Védrenne, et al., "Investigation on adaptive optics performance from propagation channel characterization with the small optical transponder," Opt. Eng. 55(11), 111611 (2016), doi: 10.1117/1.OE.55.11.111611.

[12] D.-H. Phung ; E. Samain et al. ,"Telecom and scintillation first data analysis for DOMINO: laser communication between SOTA, onboard SOCRATES satellite, and MEO optical ground station", Proc. SPIE 9739, Free-Space Laser Communication and Atmospheric Propagation XXVIII, 973909 (March 15, 2016); doi:10.1117/12.2218524.

[13] K. Saab, V. Michau, C. Petit , N. Vedrenne, P. Bério, M. A. Martinod,"Optimization of coupling between Adaptive Optics and Single Mode Fibers", CHARA 2016, Nice March 14-16 2016

[14] L. Andrews, R. Phillips, R. Crabbs, D. Wayne, T. Leclerc and P. Sauer, Creating a C2n profile as a function of altitude using scintillation measurements along a slant path, Proc. of SPIE (2012).